ORGANIC SUPERCONDUCTIVITY - II

Organic superconductors part of a generic phase diagram

The Copenhagen group led by Klaus Bechgaard and experienced with the chemistry of selenium succeeded in the synthesis of a new series of conducting salts all based on the TMTSF molecule namely, $(TMTSF)_2X$ where X is an inorganic mono-anion with various possible symmetry, spherical (PF_6, AsF_6, SbF_6, TaF_6), tetrahedral (BF_4, ClO_4, ReO_4) or triangular (NO_3) [24],*see* fig(4). All these compounds but the one with $X=ClO_4$ did reveal an insulating ground state under ambient pressure.

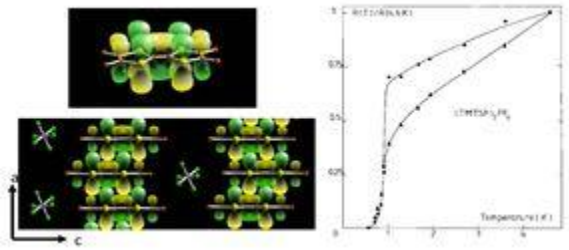

Figure 4: Side view of the TMTSF molecule (yellow and red dots are selenium and carbon atoms respectively, hydrogens not shown) and $(TMTSF)_2PF_6$ quasi 1D structure along the *b* axis, *courtesy* of J.Ch. Ricquier, IMN, Nantes (left) . First observation of superconductivity in $(TMTSF)_2PF_6$ under a pressure of 9 kbar [29]. The resistance of two samples is normalized to the 4.5 K value (right).

What is so special with $(TMTSF)_2PF_6$, the prototype of the so-called Bechgaard salts? Unlike previously investigated TTF-TCNQ, it is the magnetic origin of the ambient pressure insulating state [26] contrasting with the Peierls-like ground states discovered previously in charge transfer compounds. The ground state of $(TMTSF)_2PF_6$ turned out to be a spin density wave state similar to the predictions made by Lomer [27] in 1962 and by Overhauser [28] for metals. It is the onset of itinerant antiferromagnetism which opens a gap at Fermi level. Since the Fermi surface is nearly planar, the exchange gap develops over the whole surface (although the *SDW* phase still retains small pockets of carriers, *see* [30] for references). The magnetic origin of the insulating ground state of $(TMTSF)_2PF_6$ was thus the first experimental hint for the prominent role played by correlations in these organic conductors.
Superconductivity of $(TMTSF)_2PF_6$ occurred at 1K as shown by transport, fig(4), once the *SDW* insulating ground state could be suppressed increasing the transverse overlap between molecular stacks under a pressure of about 9 kbar [29]. AC susceptibility measurements performed on the same material detected an anomaly at T_c indicative of a transition into a diamagnetic state [31]. A confirmation of the bulk nature of organic superconductivity has been given subsequently by the observation of shielding and Meissner signals in $(TMTSF)_2PF_6$ [32].

The synthesis of the superconducting compound $(TMTSF)_2PF_6$ allowed to establish a link between this compound and the isostructural family comprising the sulfur molecule with the same series of monoanions discovered earlier. Thanks to an intensive study under pressure, it was realized that $(TMTTF)_2X$ and

$(TMTSF)_2X$ salts both belong to a common class of materials forming the generic $(TM)_2X$ phase diagram [33], fig(5).

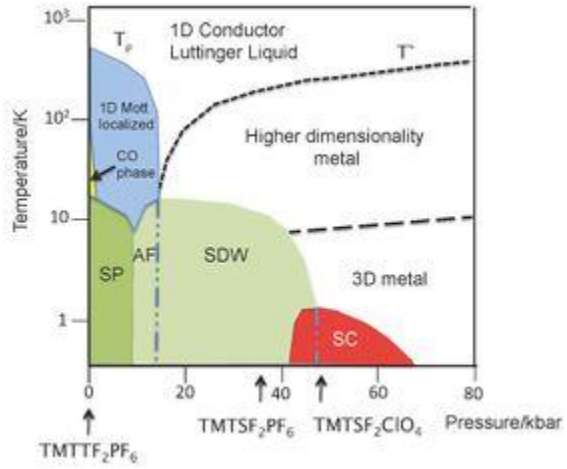

Figure 5: Generic phase diagram for the $(TM)_2X$ family [33] based on the sulfur compound $(TMTTF)_2PF_6$under ambient pressure taken as the origin for the pressure scale. Phases in yellow, green, light green and red colors are long range ordered, Charge Order (CO), Spin Peierls (SP), Magnetic phases Neel antiferromagnet and Spin Density Wave phase and Superconductivity respectively. There exists a small pressure window around 45 kbar in this generic diagram where SC coexists with SDW according to reference [36, 37, 38]. T_ρ marks the onset of 1D charge localization which ends around 15 kbar at the dashed double-dotted line. The (TL)1D to 2D deconfinement occurs at $T_\star$. The dashed line between 2D and 3D regimes defines the upper limit for low temperature 3D coherent domain.

In particular, $(TMTTF)_2PF_6$, although the most insulating compound of the phase diagram can be made superconducting at low temperatures under a pressure of 45 kbar [34, 35]. The study of this generic phase diagram has in turn greatly contributed to the experimental exploration of 1D physics and to the comparison with the theory.

$(TM)_2X$ conductors exhibit a band filling commensurate with the underlying 1D lattice due to the 2:1 stoichiometry imposing half a hole per TM molecule. However, non-uniformity of the intermolecular spacing had been noticed from the early structural studies of $(TMTTF)_2PF_6$ crystal [39] due to the periodicity of the anion packing being twice the periodicity of the molecular packing. This non-uniformity provides a dimerization of the intrastack overlap quite significant in the sulfur series (prominent 1/2 filling Umklapp scattering) and still present in the members of the $(TMTSF)_2PF_6$ series. An important consequence of the commensurate situation for $(TM)_2X$ materials is the existence of two localization channels either due to electron-electron Umklapp scattering with momentum transfer $4k_F$ (two particles scattering) or to $8k_F$ (four particles scattering) corresponding to half or quarter-filled bands respectively [40, 41]. Consequently, both Umklapp mechanisms compete for the establishment of the 1D charge gap Δ_ρ, 1/4 and 1/2 filling Umpklapp scatterings leading to charge ordered and Mott insulators respectively [42].

On the left side of the generic diagram on fig(5) a phase transition towards a long range charge ordered (CO) insulating phase has been observed. This phase at low temperature has been ascribed, according to NMR data, to the onset of a charge disproportionation between molecules on the molecular chains [43]. Increasing pressure, spins localized on dimers of molecules couple to the lattice and give rise to a spin-Peierls ground state evolving through a quantum critical point around 10 kbar [44] into a Néel antiferromagnetic phase and subsequently a spin density wave state under pressure which have been extensively studied by transport [45] and AFMR [46].

Moving toward the right side of the diagram, the onset of charge localization below T_ρ (i.e, 1D confinement) decreases under pressure as a result of an interplay between the Mott localization and the interchain coupling (increasing under pressure) which tends to bypass the correlation-induced localization. Once the localization gap vanishes, 1D confinement ceases and the existence of a quasi-1D Fermi surface becomes meaningful[41, 47, 48]. In some respects the deconfinement observed under pressure around 15 kbar on fig(5) is the signature for a crossover from strong to weak coupling in the generic phase diagram. The Néel phase turns into an ordered weak antiferromagnetic spin density wave phase (*SDW*) above the deconfinement pressure of about 15 kbar.

The temperature $T_\star$ where the $c_\star$-axis transport switches from an insulating to a metallic temperature dependence[49] corresponds to a cross-over between two regimes, see fig(5); a high temperature regime in which the finite QP weight at Fermi energy is smaller than the regular metallic value (possibly a TL liquid in the 1D case described below). $T_\star$ is highly pressure dependent and can be as small as 20 K or so, a value much smaller than the one expected for the bare $t_\perp$ of order 200 K. $T_\star$ would recover the value of the bare coupling only under infinite pressure.

Regarding the upper part of the diagram on fig(5) transport in $(TM)_2X$ has been interpreted in terms of the Tomonaga-Luttinger liquid model for a commensurate conductor. A metal-like behaviour of the longitudinal resistance is still observed as long as T is larger than Δ_ρ leading to a resistance displaying a power law $\rho(T)\approx T_\theta$ ($\theta>0$). Experimental studies have revealed such a metallic behaviour for the resistance either in $(TMTTF)_2X$ under pressure [49, 50] or in $(TMTSF)_2X$ even at ambient pressure [15]. What has been found is a sublinear exponent, namely $\theta=0.93$ for the constant volume temperature dependence of the $(TMTSF)_2PF_6$ resistance [49, 50]. In the vicinity of $T_\star$, this power law evolves toward a constant value in line with a Fermi liquid picture.

When quarter-filled Umklapp scattering prevails at high temperature $\theta=16K_\rho-3$ and consequently $K_\rho=0.23$ according to the data of $(TMTSF)_2PF_6$ [50].

The temperature $T_\star$ where the $c_\star$-axis transport switches from an insulating to a metallic temperature dependence [49] corresponds to a cross-over between two regimes, *see* fig(5); a high temperature regime with no QP weight at Fermi energy (possibly a TL liquid in the 1D case described above) in which the QP weight increases with decreasing temperature.

A three dimensional anisotropic coherent picture prevails at low temperature in $(TMTSF)_2X$ compounds according to the Kohler's rule [51] and angular magnetoresistance oscillationsobserved in $(TMTSF)_2ClO_4$ and $(TMTSF)_2PF_6$ under pressure [52, 53, 54, 55]. In addition, optical reflectance data of light polarised along $c_\star$ support the existence for $(TMTSF)_2ClO_4$ of a weak Drude behaviour in the liquid helium temperature

domain when $k_BT<t_{\perp c}$ [56]. However, the upper limit for the temperature domain of 3D coherence has been established comparing the temperature dependence of the resistivity along *a* and $c\star$. This 2D to 3D crossover domain is defined by the temperature above which the temperature dependencies of both components of transport are no longer identical [57]. The 3D coherence regime is displayed on the generic diagram of fig(5). The low temperature limit of the metallic phase will be discussed in section(Organic Superconductivity#Antiferromagnetic fluctuations, spin and charge sectors).

Organic Superconductivity

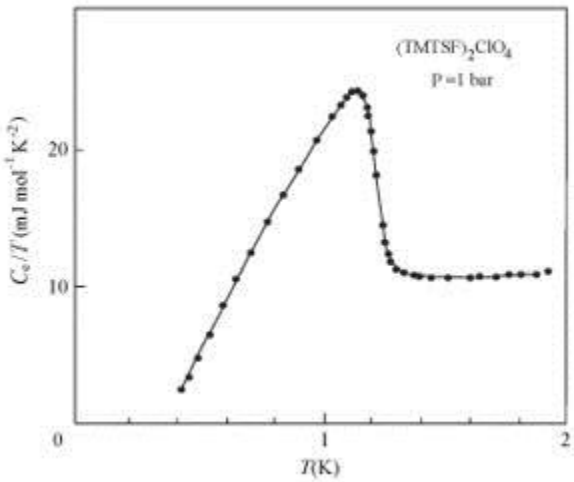

Figure 6: Electronic contribution to the specific heat of $(TMTSF)_2ClO_4$, plotted as C_e/T versus T, according to ref[59].

Although superconductivity in organic conductors has been first stabilized under pressure, more detailed investigations of this phenomenon have been conducted in $(TMTSF)_2ClO_4$, the only compound of the 1D-Bechgaard salts series exhibiting superconductivity at ambient pressure below 1.2 K. Evidences for superconductivity in $(TMTSF)_2ClO_4$ came out from transport [58], specific heat measurements [59] and Meissner flux expulsion [60].

The electronic contribution to the specific heat of $(TMTSF)_2ClO_4$ in a C_e/T *vs* T plot, fig(6), displays a very large anomaly around 1.2 K [59]. The total specific heat obeys the classical relation in metals $C/T=\gamma+\beta T^2$, where the Sommerfeld constant for electrons γ = 10.5 mJ $mol^{-1}K^{-2}$, corresponding to a density of states at the Fermi level $N(E_F)$ = 2.1 states $eV^{-1}mol^{-1}$ for the two spin directions [59]. The specific heat jump at the transition amounts then to $\Delta C_e/\gamma T_c=1.67$, *i.e.* only slightly larger than the BCS ratio for a *s*-wave superconductor. Therefore, the specific heat data and the comparison between the value of the density of states derived specific heat Pauli susceptibility [61] lend support to a weak coupling Fermi liquid picture (at least in the low temperature range) [47]. The first critical field H_{c1} obtained from the Meissner magnetization curves at low temperature read, 0.2,1 and 10 Oe along axes *a*, *b'*and $c\star$ respectively. Following the values for the second critical fields H_{c2}derived either from the Meissner experiments and the knowledge of the thermodynamical field [60] or from a direct measurements of transport, superconductivity can be considered to be in the extreme type II limit. The Ginzburg-Landau parameter κ can even overcome 1000 when the field is along *a* due to the

weak interchain coupling in these Q1D conductors making the field penetration very easy for the parallel configuration of the external field. An interpretation for the critical fields assuming the pure limit of type II superconductors has been suggested in 1985 [62]. This proposal was based on the calculation of the microscopic expressions for the effective mass tensor in the Ginzburg-Landau equation near T_c [63].

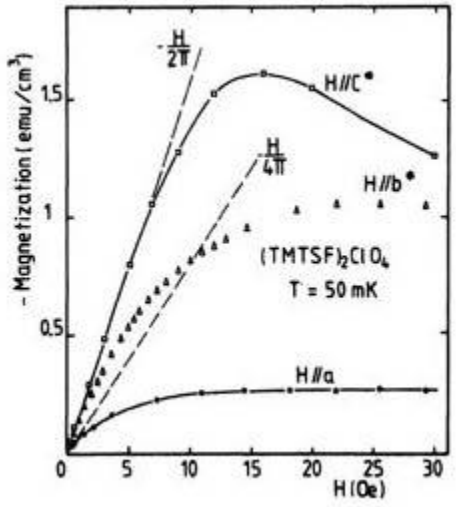

Figure 7: Diamagnetic shielding of $(TMTSF)_2ClO_4$ at T=0.05K for magnetic fields oriented along the three crystallographic axes, from ref [60].

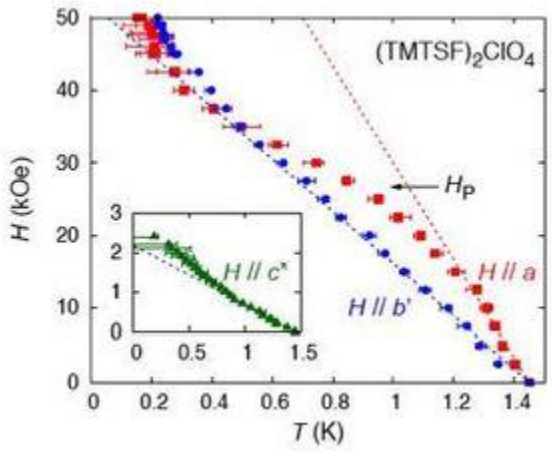

Figure 8: Critical fields of $(TMTSF)_2ClO_4$ determined from $T_{c,onset}$ for the three principal axes with an indication for the Pauli limit at low temperature after [64, 65].

Given the experimental determination of the critical field derivatives near T_c of $(TMTSF)_2ClO_4$ [64, 65], dH_{ac2}/dT = 67.5kOe/K, $dH_{b'c2}/dT$ = 36.3kOe/K, and dH_{cc2}/dT = 1.39kOe/K, Eqs.(1-3) lead to band parameters t_a:t_b:t_c = 1200, 300 and 6K respectively are derived when critical fields derivatives are determined from $T_{c,onset}$ for the three principal axes after [64, 65].

Pairing mechanism in organic superconductivity

For several reasons one is entitled to believe that the pairing mechanism in organic superconductivity may differ from the regular electron-phonon driven pairing in traditional superconductors. First, superconductivity of quasi one dimensional Bechgaard salt shares a common border with magnetism as displayed on the generic diagram, see fig(5). Second, strong antiferromagnetic fluctuations in the normal state above T_c in the vicinity of the *SDW* phase provide the dominant contribution to the nuclear hyperfine relaxation and are also controlling the linear temperature dependence of electronic transport. Some experimental results point to the existence of a non conventional pairing mechanism. They will be summarized below.

Non magnetic defects

A basic property of the BCS superconducting *s*-wave function is the time reversal symmetry of the Cooper pairs. Hence no pair breaking is expected from the scattering of electrons against spinless impurities [66]. Experimentally, this property has been verified in non-magnetic dilute alloys of *s*-wave superconductors and brought a strong support for the BCS model of conventional *s*-wave superconductors. However, the condition for time reversal symmetry is no longer met for the case of *p*-wave pairing. Consequently,T_c for these superconductors should be strongly affected by any non-magnetic scattering. It is actually the extreme dependence of the critical temperature of Sr_2RuO_4 [67] on non-magnetic disorder which has provided a strong support in favour of triplet superconductivity in this compound. It is also the remarkable sensitivity of organic superconductivity to irradiation detected in the early years [68, 69] which led Abrikosov to suggest the possibility of triplet pairing in these materials [70].

A more recent investigation of the influence of non magnetic defects on organic superconductivity has been conducted following a procedure which rules out the addition of possible magnetic impurities as it can be the case for X-ray irradiated samples. Non magnetic defects can be introduced in a controlled way either by fast cooling preventing the complete ordering of the tetrahedral ClO_4 anions or by slow cooling the solid solution $(TMTSF)_2(ClO4)_{(1-x)}ReO_{4x}$.

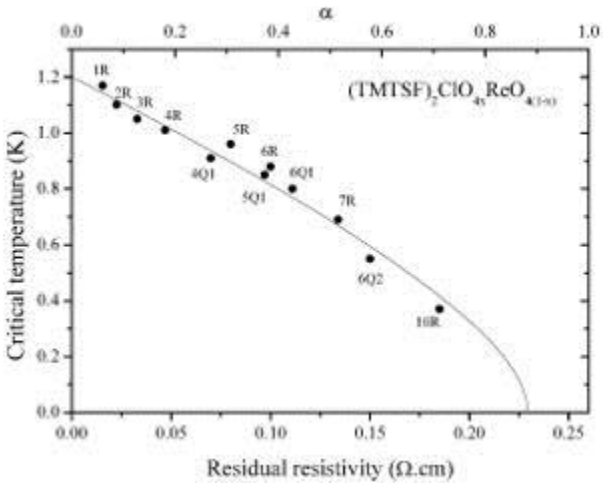

Figure 9: Phase diagram of $(TMTSF)_2(ClO4)_{(1-x)}ReO_{4x}$ governed by non magnetic disorder according to ref[71]. All circles refer to very slowly cooled samples in the R-state (the so-called relaxed state) with different ReO_{-4} contents. The sample

with $\rho_0=0.27(\Omega cm)^{-1}$ is metallic down to the lowest temperature of the experiment. The continuous line is a fit of the data with the Digamma function and $T_{c0}=1.23K$.

As displayed on fig(9), T_c in the solid solution is suppressed and the suppression can be related to the enhancement of the elastic scattering in the normal state. The data on fig9 show that the relation T_c versus ρ_0 follows the theory proposed for the pair breaking by magnetic impurities in conventional superconductors, namely

$$ln(T_{0c}T_c)=\psi(12+\alpha T_{0c}2\pi T_c)-\psi(12),(1)$$

with $\psi(x)$ being the Digamma function, $\alpha=\hbar/2\tau k_B T_{0c}$ the depairing parameter τ. The experimental data follow the latter law with a good accuracy with $T_{c0}=1.23K$.

The conventional pair breaking theory for magnetic impurities in usual superconductors has been generalized to the case of non-magnetic impurities in unconventional materials and the correction to T_c obeys the above relation [72, 73]. Since the additional scattering cannot be ascribed to magnetic scattering according to the EPR checks showing no additional traces of localized spins in the solid solution, the data in fig(9) cannot be reconciled with the picture of a superconducting gap keeping a constant sign over the whole ($\pm k_F$) Fermi surface. They require a picture of pair breaking in a superconductor with some unconventional gap symmetry.

Symmetry	s	p	d	f	g
Sensitivity to impurities		√	√	√	√
NMR Knight shift and $1/T_1$	√		√		√
Doppler shift			√	(√)	√

Figure 10: Possible gap symmetries agreeing with the different experimental results. The *d*-wave (or *g*-wave) symmetry is the only symmetry agreeing with all experiments, (yellow column on line).

The influence of non magnetic impurities on the superconducting phase implies the existence of positive as well as negative values for the *SC* order parameter. It precludes the usual case of *s*-symmetry but is still unable to discriminate between two possible options namely, singlet-*d (g)* or triplet-*p (f)* [74], *see* fig(10).

Spin susceptibility in the superconducting phase

Regarding the spin part of the *SC* wave function, a triplet pairing was first claimed in $(TMTSF)_2PF_6$ from a divergence of the critical field H_{c2} exceeding the Pauli limiting value reported at low temperature in $(TMTSF)_2PF_6$ under pressure when *H* is applied along the *b'* or *a* axes [75] and from the absence of any change in the ^{77}Se Knight shift at T_c [76].

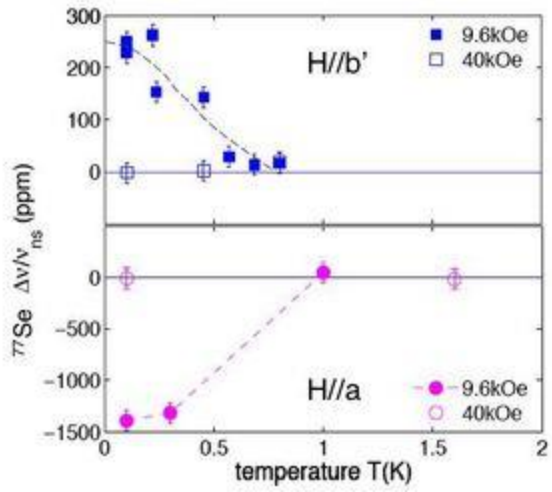

Figure 11: ^{77}Se Knight shift vs T for $(TMTSF)_2ClO_4$, for $H//b'$ and a, according to reference [77]. The sign of the variation of Knight shift at T_c depends on the sign of the hyperfine field. A variation is observed only under low magnetic field. The difference of T_c for the two field orientations is related to the anisotropy of H_{c2}. The field of $4T$ is still lower than the critical field derived from the onset of the resistive transition ($H_{c2}\approx 5T$).

However more recent experiments performed at fields lower than those used in reference [76] for the work on $(TMTSF)_2PF_6$ did reveal a clear drop of the ^{77}Se Knight shift below $T_c$in the compound $(TMTSF)_2ClO_4$ [77]. These new data provided a conclusive evidence in favour of singlet pairing, fig(11). In addition, a steep increase of the spin lattice relaxation rate versus magnetic field for both field orientations $\|a$ and b' provided evidence for a sharp cross-over or even a phase transition occurring at low temperature under magnetic field between the low field d-wave singlet phase and a high field regime exceeding the paramagnetic limit H_p being either a triplet-paired state [78, 79] or an inhomogenous Fulde-Ferrell-Larkin-Ovchinnikov state [80, 73].

Magneto calorimetric studies

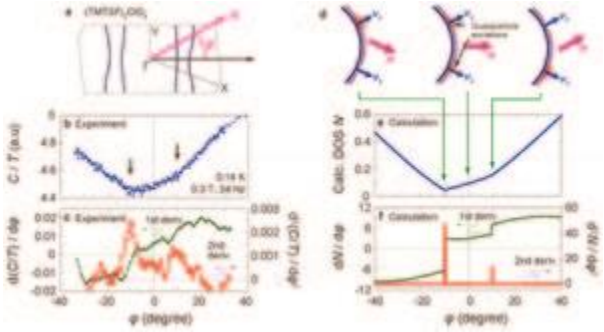

Figure 12: a- Fermi surface of $(TMTSF)_2ClO_4$ at low temperature in the presence of anion ordering [81]. b- Angular dependence of $C(\phi)$ at 0.14 K and 0.3 T according to ref[82]. c- First and second derivatives of the data displayed on a. d- Sketch of the influence of a magnetic field on the quasi particle DOS. The contribution of Doppler-shifted quasi-particles to the DOS is minimum when the magnetic field is parallel to $\mathbf{v}_F$ at one of the nodes (left or right) . e and f- Simulations of the specific heat in

the vicinity of the angle ϕ=0using the band structure on fig(12a). Arrows correspond to the different orientations of the magnetic field as shown on fig(12).

The response of superconductivity to non magnetic impurities and the loss of spin susceptibility at T_c should be sufficient to qualify the *d*-wave alternative as the likely one among the various possibilities displayed on fig(10). In such a case, nodes of the gap should exist on the Fermi surface and could be located. This has been made possible via a measurement of the quasi particle density of states in the superconducting phase performed in an oriented magnetic field [82], *see* figs (12 b and c). This experiment is based on a Volovik's important remark [83] that for superconductors with line nodes, most of the density of states in their mixed state under magnetic field comes from the superfluid density far outside the vortex cores. The energy of QP's in the superfluid density rotating around the vortex core with the velocity $v_s(\perp H)$ is Doppler-shifted by the magnetic field and reads,

$$\delta\omega \propto \mathbf{v}_s \cdot \mathbf{v}_F(\mathbf{k}) \quad (2)$$

where $\mathbf{v}_F(\mathbf{k})$ is the Fermi velocity at the **k** point on the Fermi surface. The Doppler shift can contribute to the DOS in the superconducting state as long as it remains smaller than the superconducting energy gap, *i.e* only for those **k** states located in the vicinity of gap nodes on the Fermi surface. Hence, the contribution of the Doppler shift is minimum when the Fermi velocity at a node and the magnetic field are parallel according to eq (2), *see* fig(12d), and should contribute to a kink in the rotation pattern of the electronic specific heat $C(\phi)$.

The Doppler shift has already been used extensively in the case of 2D superconductors expected to reveal line nodes probing the thermal conduction or the specific heat while the magnetic field is rotated in the basal plane [84,85]. For such 2D conductors $\mathbf{v}_F(\mathbf{k})$ is usually colinear with **k**. Therefore, the angular resolved specific heat (or thermal conductivity) enables to reveal the positions of the gap nodes according to the angles corresponding to minima of specific heat (thermal conductivity) [84].

The situation is somewhat peculiar for Q1D Fermi surface. There, anomalies in the rotation pattern of C_v are expected at angles ϕ_n between H and $\mathbf{v}_F(\mathbf{k}_n)$ where $\mathbf{k}_n$ corresponds to a nodal position on the Fermi surface. A simple model has been used to understand the data of angular resolved C_v of $(TMTSF)_2ClO_4$ [82]. The rotation pattern has been modeled by,

$$N(\phi) \propto H/H_{c2}(\phi) \sqrt{\Sigma_n A_n |sin(\phi-\phi_n)|} \quad (3)$$

where the first factor reproduces the anisotropic character of the critical field in the basal plane while the weighted summation over angles accounts for the existence of nodes at angles ϕ_n between the magnetic field and the special $\mathbf{k}_n$ points where the Fermi velocity is parallel to H. The experimental observation of a rotation pattern at low field and low temperature which is non symmetrical with respect to the inversion of ϕ and the existence of kinks for $C(\phi)$ at $\phi=\pm 10_o$ on fig (12b) have been taken as the signature of line nodes [82]. According to the band structure calculation the location of the nodes on the Fermi surface becomes $k_y \sim \pm 0.25 b_*$. As far as the Pauli limitation is concerned, the superconducting phase diagram of $(TMTSF)_2ClO_4$established by thermodynamic experiments indicates a value for the thermodynamic H_{c2} along a of 2.5 T for $H \| a$ much smaller than the expected value of 7.7 T for the orbital limitation derived from the measurement of the temperature derivative of H_{c2} close to $T_c$for a clean type II superconductor [62]. On the other hand, along the two transverse directions orbital limitation is at work [82]. The domain of field above the paramagnetic limit up to H_{c2} derived from resistivity data where the specific heat recovers its normal state value requires

further experimental investigations but it might be the signature of some *FFLO* phase as suggested by A. Lebed recently [86, 87, 88].

Antiferromagnetic fluctuations, spin and charge sectors

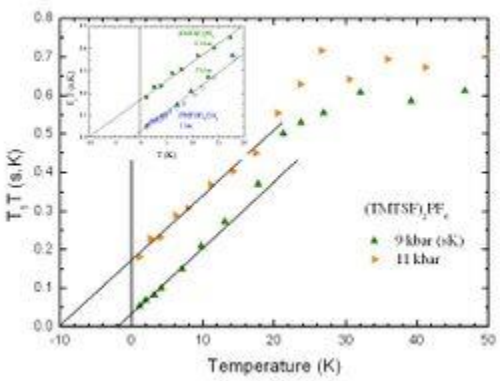

Figure 13: Plot of the nuclear relaxation versus temperature according to the data of ref[89]. A Korringa regime, T_1T = const is observed down to 25K. The 2D AF regime is observed below $\approx 15K$ and the small Curie-Weiss temperature of the 9 kbar run is the signature of the contribution of quantum critical fluctuations to the nuclear relaxation. The Curie-Weiss temperature becomes zero at the QCP. These data show that the QCP should be slightly below 9 kbar with the present pressure scale. The inset shows that the organic superconductor $(TMTSF)_2ClO_4$ at ambient pressure is very close to fulfill quantum critical conditions.

The metallic phase of $(TMTSF)_2PF_6$ in the 3D coherent regime when pressure is in the neighbourhood of the critical pressure $P_c$behaves in way far from what is expected for a Fermi liquid.
The canonical Korringa law , $1/T_1T \propto \chi_2(q=0,T)$, is well obeyed at high temperature say, above 25 K, but the low temperature behaviour deviates strongly from the standard relaxation in paramagnetic metals. As shown on fig (13) an additional contribution to the relaxation rate emerges in top of the usual Korringa relaxation. This additional contribution rising at low temperature has been attributed to the onset of antiferromagnetic fluctuations in the vicinity of P_c [90, 91, 92]. On the other hand in the low temperature regime the relaxation rate follows a law such as $T_1T=C(T+\Theta)$ as shown on fig(13). This is the Curie-Weiss behaviour for the relaxation which is to be observed in a 2D fluctuating antiferromagnet [93, 94, 95, 96]. The positive Curie-Weiss temperature Θ which provides the energy scale of the fluctuations is zero when pressure is equal to P_c (the quantum critical conditions). When Θ becomes large comparable to T, the standard relaxation mechanism is recovered even at low temperature in agreement with the very high pressure results [97].
The inelastic scattering in transport reveals at once a strong linear term at low temperature evolving to quadratic in the high temperature regime with a general tendency to become quadratic at all temperatures when pressure is way above the critical pressure P_c [90], *see* fig(5).

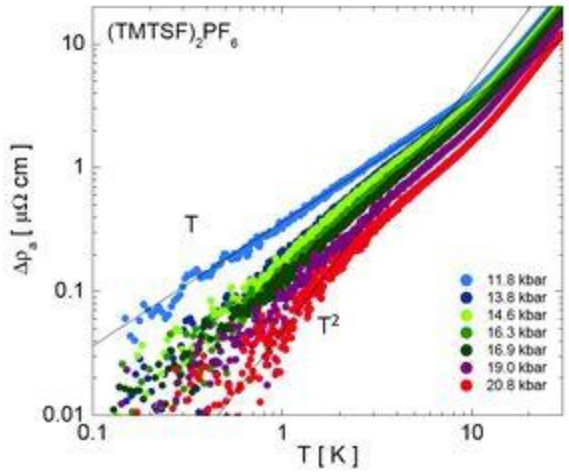

Figure 14: A log-log plot of the inelastic longitudinal resistivity of $(TMTSF)_2PF_6$ below 20 K, according to ref[90].

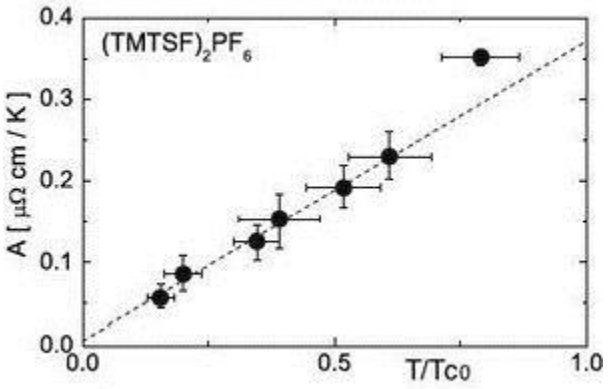

Figure 15: Coefficient A of linear resistivity as a function of T_c plotted versus T_c/T_{c0} for $(TMTSF)_2PF_6$. T_c is defined as the midpoint of the transition and the error bars come from the 10% and 90% points withT_{c0}=1.23K under the pressure of 8 kbar which provides the maximum T_c in the *SDW*/*SC* coexistence regime.The dashed line is a linear fit to all data points except that at T_c=0.87K, according to ref[90].

The existence of a linear temperature dependence of the resistivity is *at variance* with the sole T^2 dependence expected from the electron-electron scattering in a conventional Fermi liquid. This is clearly seen on a log-log plot of the resistivity versus T, *see*fig(14). Furthermore, the investigation of both transport and superconductivity under pressure in $(TMTSF)_2PF_6$ has established a correlation between the amplitude of the linear in temperature dependence of the resistivity and the value of T_c as displayed on fig(15) suggesting a common origin for the inelastic scattering of the metallic phase and pairing in the *SC* phase $(TMTSF)_2PF_6$[90] as discussed in the next section.

Discussions and perspectives

The close proximity between antiferromagnetism and superconducting ground states of $(TM)_2X$ superconductors and the deviation of the metallic phase from the traditional Fermi liquid behaviour have been

recognized as early as the beginning eighties. The possibility for a pairing mechanism involving carriers on neighbouring chains in these quasi 1D conductors avoiding the Coulomb repulsion has been proposed by V. Emery in the context of the exchange phonon mechanism [98]. Shortly after, Emery and coworkers introduced the possibility that antiferromagnetic fluctuations play a role in the pairing mechanism [99, 100] but concluded that superconductivity could not emerge from pairing on the same organic chain. The exchange of spin fluctuations between carriers on neighbouring chains was thus proposed [99] to provide the necessary glue for pairing in analogy with the exchange of charge density waves proposed by Kohn and Luttinger [101] in the context of a new pairing mechanism in low dimensional conductors.

L. Caron and C. Bourbonnais [102, 103] extending their theory for the generic $(TM)_2X$ phase diagram to the metallic domain made the proposal for a gap equation with singlet superconductivity based on an interchain magnetic coupling with an attraction deriving from an interchain exchange interaction overcoming the on-stack Coulomb repulsion. Taking into account the interference between the diverging Cooper and Peierls channels the renormalization treatment of Q-1-D conductors received more recently a significant improvement [104]. Within the framework of a weak-coupling limit the problem of the interplay between antiferromagnetism and superconductivity in the Bechgaard salts has been worked out using the renormalization group (RG) approach [74, 96] as summarized below taking into account only the 2D problem. The RG integration of high energy electronic degrees of freedom was carried out down to the Fermi level, and leads to a renormalization of the couplings at the temperature T [96, 104, 105]. The RG flow superimposes the $2k_F$ electron-hole (density-wave) and Cooper pairing many-body processes which combine and interfere at every order of perturbation. As a function of the `pressure' parameter $t'_\perp$ *i.e* the unnesting interstacks coupling, a singularity in the scattering amplitudes signals an instability of the metallic state toward the formation of an ordered state at some characteristic temperature scale. At low $t'_\perp$, nesting is sufficiently strong to induce a *SDW* instability in the temperature range of experimental $T_{SDW} \sim 10-20$K. When the antinesting parameter approaches the threshold $t'_{*\perp}$ from below ($t'_{*\perp} \approx 25.4$ K, using the above parameters), T_{SDW} sharply decreases and as a result of interference, *SDW* correlations ensure Cooper pairing attraction in the superconducting *d*-wave (*SCd*) channel. This gives rise to an instability of the normal state for the onset of *SCd* order at the temperature T_c with pairing coming from antiferromagnetic spin fluctuations between carriers of neighbouring chains. Such a pairing model is actually supporting the conjecture of interchain pairing in order for the electrons to avoid the Coulomb repulsion made by V. Emery in 1983 and 1986 [98, 99].

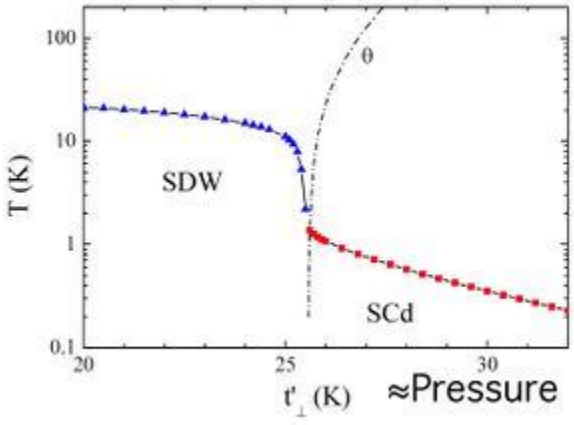

Figure 16: Calculated phase diagram of the quasi-one dimensional electron gas model from the renormalization group method at the one-loop level [96]. Θ and the dash-dotted line defines the temperature region of the CW behavior for the inverse normalized *SDW* response function

The calculated phase diagram fig(16) with reasonable parameters taking $g_1=g_2/2\approx 0.32$ for the backward and forward scattering amplitudes respectively and $g_3\approx 0.02$ for the longitudinal Umklapp scattering term captures the essential features of the experimentally-determined phase diagram of $(TMTSF)_2PF_6$ [92, 96], fig(5). Sedeki *et-al* [106] have proceeded to an evaluation of the imaginary part of the one-particle self-energy which provides access to the electron-electron scattering rate τ^{-1}. In addition to the regular Fermi-liquid component which goes as T^2 low frequency spin fluctuations yield $\tau^{-1}=aT\xi$, where a is constant and the antiferromagnetic correlation length $\xi(T)$ increases according to $\xi=c(T+\Theta)^{-1/2}$ as $T\rightarrow T_c$, where Θ is the temperature scale for spin fluctuations [106]. It is then natural to expect the Umklapp resistivity to contain (in the limit $T\ll\Theta$) a linear term AT besides the regular BT^2, whose magnitude would presumably be correlated with T_c, as both scattering and pairing are caused by the same antiferromagnetic correlations. The observation of a T-linear law for the resistivity up to 8K in $(TMTSF)_2PF_6$ under a pressure of 11.8 kbar as displayed on fig(14) is therefore consistent with the value of $\Theta=8K$ determined from NMR relaxation at 11 kbar on fig(13).

To conclude, both experimental and theoretical views point the contribution of electron correlations to the superconducting pairing problem. The extensive experimental evidence in favor of the emergence of superconductivity in the $(TM)_2X$ family next to the stability threshold for antiferromagnetism has shown the need for a unified description of all electronic excitation that lies at the core of both density-wave and superconducting correlations. In this matter, the recent progresses achieved by the renormalization group method for the 1D-2D electron gas model have resulted in predictions about the possible symmetries of the superconducting order parameter when a purely electronic mechanism is involved, predictions that often differ from phenomenologically based approaches to superconductivity but are in fair agreement with the recent experimental findings. In this respect reexaminations of the superconducting state, specific heat, thermal conductivity,etc,...are highly demanded.

What is emerging from the work on these prototype 1D organic superconductors is their very simple electronic nature with only a single band at Fermi level, no prominent spin orbit coupling and extremely high chemical purity and stability.

They should be considered in several respects as model systems to inspire the physics of the more complex high $T_c$superconductors, especially for pnictides and electron-doped cuprates. Most concepts discovered in these simple low dimensional conductors should be very useful for the study of other low dimensional systems such as carbon nanotubes or artificial 1D structures, etc,.....

The pairing mechanism behind organic superconductivity is likely different from the proposal made by Little but it is nevertheless a phonon-less mechanism, at least in $(TM)_2X$ superconductors.

In conclusion, organic superconductivity has been discovered in the prototype Bechgaard salt $(TMTSF)_2PF_6$ but several other fascinating aspects of the physics of 1D conductors are worth mentioning

namely, the magnetic field confinement discovered in the 1D's leading to the phenomenon of field induced spin density wave phases [107, 108, 109] and the quantization of the Hall effect in these phases [110, 111, 112]. Furthermore, the angular dependent magnetoresistance closely related to these anisotropic conductors [53, 113], (*see* [114] for a recent survey), the so-called Lebed-Osada-Danner-Chaikin oscillations in $(TMTSF)_2X$ provide a nice illustration for the new features of the quasi-1D conductors [115].

Source : http://www.scholarpedia.org/article/Organic_Superconductivity